

# The Ly $\alpha$ Forest Around High Redshift Galaxies

M. Bruscoli<sup>1</sup>, A. Ferrara<sup>2</sup>, S. Marri<sup>2</sup>, R. Schneider<sup>3</sup>, A. Maselli<sup>1</sup>,  
E. Rollinde<sup>4</sup> & B. Aracil<sup>4</sup>

<sup>1</sup>*Dipartimento di Astronomia, Università degli Studi di Firenze, L.go E. Fermi 2, 50125 Firenze, Italy*

<sup>2</sup>*SISSA/International School for Advanced Studies, Via Beirut 2-4, 34014 Trieste, Italy*

<sup>3</sup>*Osservatorio Astrofisico di Arcetri, L.go E. Fermi 5, 50125 Firenze, Italy*

<sup>4</sup>*Institut d'Astrophysique de Paris, 98bis Boulevard d'Arago, 75014 Paris, France*

23 March 2018

## ABSTRACT

Motivated by the relative lack of neutral hydrogen around Lyman Break Galaxies deduced from recent observations, we investigate the properties of the Ly $\alpha$  forest around high redshift galaxies. The study is based on improved numerical SPH simulations implementing, in addition to standard processes, a new scheme for multiphase and outflow physics description. Although on large scales our simulations reproduce a number of statistical properties of the IGM (because of the small filling factor of shock-heated gas), they underpredict the Ly $\alpha$  optical depth decrease inside 1 Mpc  $h^{-1}$  of the galaxies by a factor of  $\approx 2$ . We interpret this result as due to the combined effect of infall occurring along the filaments, which prevents efficient halo gas clearing by the outflow, and the insufficient increase of (collisional) hydrogen ionization produced by the temperature increase inside the hot, outflow-carved bubble. Unless an observational selection bias is present, we speculate that local photoionization could be the only viable explanation to solve the puzzle.

**Key words:** cosmology: theory - cosmological simulations, intergalactic medium, quasar spectra

## 1 INTRODUCTION

Galaxies form from the intergalactic medium (IGM), process such gas into stars, and possibly re-eject a fraction of it, enriched by nucleosynthetic products, back into the intergalactic space via powerful supernova-driven outflows (Mac Low & Ferrara 1999; Ferrara, Pettini & Shchekinov 2000; Madau, Ferrara & Rees 2001; Scannapieco, Ferrara & Madau 2002; Theuns *et al.* 2002). The energy deposition connected to these processes is expected to leave at least some detectable imprints on the physical state of the IGM. Thus, it is conceivable that such signatures can be studied through QSO absorption line experiments. Naively, the presence of hot outflowing gas should result primarily in two effects: [i] a decrease of the gas density and [ii] an increase of the temperature caused by shock-heating (acting in conjunction with photo-heating by the UV background) in a large (several hundreds kpc) region around the perturbing galaxy. Both these occurrences would imply an increasingly more transparent Ly $\alpha$  forest when approaching the galaxy, *i.e.* a galactic proximity effect. Quantitative confirmation of this scenario has faced tremendous difficulties, standing the complications of the physics of star formation, explosions and metal mixing in multiphase media. Hence, most simula-

tions to date had to rely on *ad hoc* recipes for such processes. Nevertheless, these ideas have stimulated the first challenging observations aimed at detecting the imprints of galaxy-IGM interplay. Adelberger *et al.* (2002, A02) obtained high resolution spectra of 8 bright QSOs at  $3.1 < z < 4.1$  and spectroscopic redshifts for 431 Lyman-break galaxies (LBGs) at lower redshifts. By comparing the positions of the LBGs with the Ly $\alpha$  absorption lines in QSO spectra, indeed they conclude that within  $\approx 0.5h^{-1}$  (comoving) Mpc of the galaxies little H I is present; on the contrary, between 1 and  $5h^{-1}$  Mpc an H I excess with respect to the IGM mean is detected. This simple interpretation might be at odd with the results of a VLT/UVES study of the Ly $\alpha$  forest in the vicinity of the LBG MS1512-cB58 showing the opposite trend (Savaglio *et al.* 2002), *i.e.* an absorption excess close to the galaxy.

Numerical simulations have also noticeable difficulties reproducing A02 results as discussed by Croft *et al.* (2002) and Kollmeier *et al.* (2002); however, these studies lack a self-consistent treatment of multiphase gas structure and/or outflow dynamics. Here we revisit A02 results through SPH simulations (Marri *et al.* 2003) that implement a new scheme for multiphase hydrodynamics and, more importantly, a physically meaningful outflow treatment; the full description of

the code and of the tests made are given in Marri & White (2002). We then derive synthetic absorption line spectra along lines of sight randomly traced through the simulation box at  $z \approx 3$  and compare them directly with A02 data to investigate galactic feedback effects on the IGM.

## 2 SIMULATIONS AND DATA ANALYSIS

We have performed hydrodynamic simulations for a  $\Lambda$ CDM cosmological model with  $\Omega_0 = 0.3$ ,  $\Omega_\Lambda = 0.7$ ,  $\Omega_b = 0.04$  and  $h = 0.7 \text{ km s}^{-1} \text{ Mpc}^{-1}$ . The initial power spectrum is cluster-normalized ( $\sigma_8 = 0.9$ ); periodic boundary conditions are adopted. We first obtained a set of low-resolution runs ( $64^3$  particles for both gas and dark matter) in a  $7h^{-1}$  comoving Mpc cube; these runs serve as a guide for more computationally expensive runs and for testing purposes. We consider a first model where the IGM multiphase structure and galaxy outflows are deliberately ignored and a second one which includes a description of both these physical effects. We will refer to these runs as **sph** and **mfb**, respectively, with the same meaning (and parameters) adopted in the description of the low-resolution  $\Lambda$ CDM test problem described in Marri & White (2002). The high-resolution run, on which the main results of the present analysis are based, is a  $128^3$  particles simulation in a  $10.5h^{-1}$  comoving Mpc box. For this run we only studied the full **mfb** model.

Softening lengths are fixed both in physical and comoving coordinates as required in GADGET (Springel, Yoshida & White 2001). Gas (dark matter) gravitational softening is approximately  $6h^{-1} \text{ kpc}$  ( $8h^{-1} \text{ kpc}$ ) comoving and  $3h^{-1} \text{ kpc}$  ( $4h^{-1} \text{ kpc}$ ) physical in the high-res case and scales according to particle number and box size in the low-res run. In all runs we include the effects of a UV background produced by QSOs and filtered through the IGM, whose shape and amplitude are taken from Haardt & Madau (1996).

### 2.1 Synthetic Ly $\alpha$ forest spectra

To allow a direct comparison of simulation results with observational data we construct synthetic Ly $\alpha$  spectra from simulation outputs at redshift  $z = 3.17$  ( $z = 3.27$ ) for the low-res (high-res) runs. In the simulation box we randomly trace 60 lines-of-sight (LOS) parallel to the  $x$ -axis, each of which is discretized into  $N_{pix} = 1024$  pixels. In order to assign to each pixel a value for the hydrogen density, temperature and peculiar velocity we perform a standard SPH smoothing using the 32 closest neighbour SPH particles to the LOS pixel position. The neutral hydrogen density is derived using the code CLOUDY94<sup>1</sup> on each pixel, adopting the same UVB as in the simulation. The transmitted flux due to Ly $\alpha$  absorption in the IGM is  $\propto e^{-\tau}$ , where  $\tau$  is the optical depth along the considered LOS. The Hubble velocity  $v_H$  varies in the range  $(0, v_H^{max})$ , where the maximum value is set by the box size. The contribution to  $\tau$  at the observed frequency corresponding to  $v_H(k)$ , where  $1 \leq k \leq 1024$  is the pixel index, is given by

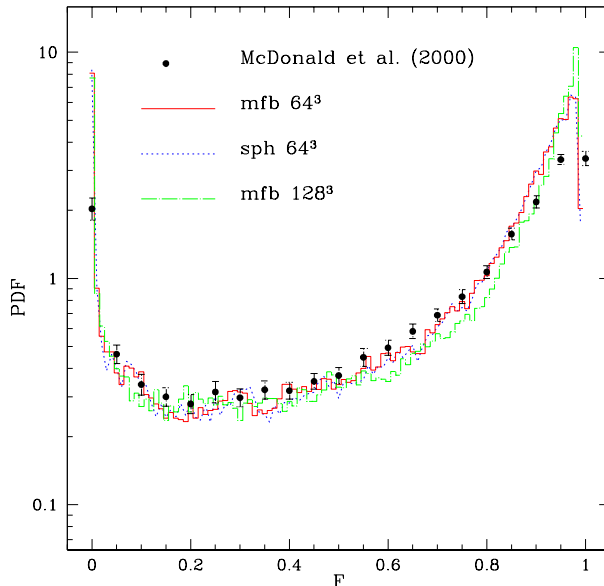


**Figure 1.** Probability distribution function of transmitted flux at  $z = 3.17$  for the low-res simulations **mfb** (solid line) and **sph** (dotted) runs, and at  $z = 3.27$  for the high resolution **mfb** run (dotted-dashed). The points represent the observational data (McDonald *et al.* 2000) at  $z = 3$ .

$$\tau[v_H(k)] = \frac{\Delta x \sigma_0 f \lambda_0}{\pi^{1/2}} \sum_{i=1}^{N_{pix}} \frac{n_{\text{HI}}(i)}{b(i)} \Phi_g[v_H(k) - v(i)], \quad (1)$$

where  $\Delta x$  is the pixel size,  $\sigma_0$  is the Ly $\alpha$  cross section,  $f$  is the Ly $\alpha$  oscillator strength,  $\lambda_0$  is the Ly $\alpha$  wavelength,  $n_{\text{HI}}(i)$ ,  $b(i)$  and  $v(i) = v_H(i) + v_{pec}(i)$  are the H I number density, the Doppler parameter, and the total velocity in the pixel  $i$ , respectively;  $\Phi_g$  is a gaussian line profile and  $v_{pec}$  is the peculiar velocity. For additional discussion on this formula, see *e.g.* Rauch, Haehnelt & Steinmetz (1997a).

To compare observations and simulations at best it is necessary to degrade the synthetic spectra to account for the uncertainties affecting the observed spectra. We perform such procedure through the following steps: *i*) continuum normalization at the highest flux value in each spectrum; *ii*) convolution with the instrumental profile; *iii*) sampling due to spectrograph spatial resolution; *iv*) addition of instrumental noise (see Rauch *et al.* 1997b; Theuns *et al.* 1998; McDonald *et al.* 2000; Petry *et al.* 2002). As most of the data we compare with are taken with the Keck/HIRES spectrograph we adopt the following instrumental characteristics: FWHM =  $8.0 \text{ km s}^{-1}$ , pixel spectral resolution  $\Delta\lambda = 0.05\text{\AA}$  and signal-to-noise ratio S/N=50. The low (high) resolution box has a wavelength extent of  $\Delta\lambda_{box} = 13.46\text{\AA}$  ( $\Delta\lambda_{box} = 20.83\text{\AA}$ ); hence, degraded spectra in the two cases are made of 269 and 417 pixels, respectively.

## 3 RESULTS

As a general sanity check of the simulations we have first confronted the simulated statistical properties of the Ly $\alpha$

<sup>1</sup> <http://nimbus.pa.uky.edu/cloudy/>

forest with the observed ones. The most obvious comparison involves the probability distribution function (PDF) of the transmitted flux. In Fig.1 we plot the PDF as a function of the flux  $\langle F \rangle = e^{-\tau}$  for the low-res (both **mfb** and **sph** runs) and high-res simulations (**mfb** case only) and compare them with the observational data of McDonald *et al.* (2000). The general agreement is quite good through all the flux range and for all three cases. The discrepancy between simulations and data at high fluxes is probably due to the uncertainties in the data continuum fitting (McDonald *et al.* 2000; Croft *et al.* 2002). Surprisingly, it appears that the inclusion of multiphase and outflow physics, not considered in the pure **sph** run, does not affect the distribution in a sensible manner. In other words, galactic outflows leave the Ly $\alpha$  forest unperturbed. This result is in agreement with that recently found by Theuns *et al.* (2002), who interpreted it as an indication that galactic outflows tend to propagate preferentially in the voids leaving the Ly $\alpha$  absorbing filaments virtually unaffected. As an additional check we have calculated the Doppler parameter,  $b$ , and the H I column density distribution, and compared them with two QSOs observations at  $z_{em} = 3.38$  and  $z_{em} = 3.17$  by Hu *et al.* (1995). The values of  $b$  and  $N_{\text{HI}}$  for each absorber in the synthetic spectra have been derived using the fitting program AUTOVP. The experimental  $b$  distribution is well reproduced both by the **sph** and **mfb** (low-res + high-res) runs at similar quality level (simulated and observed distributions peak both around  $b \sim 20 \text{ km s}^{-1}$ ). However, simulated spectra tend to slightly overproduce lines with  $10 < b < 22 \text{ km s}^{-1}$  and under-predict lines with  $25 < b < 50 \text{ km s}^{-1}$ . A similar effect has already been noted by Theuns *et al.* (1998). These authors propose a number of possible explanations for this behavior: physical (HeII reionization, radiative transfer effects), numerical (resolution) and related to data analysis (fitting procedure). Our results seem to indicate that numerical artifacts should not be the dominant factor. As for the H I column density distribution, the **mfb** case seems to reproduce the observational data for  $\log N_{\text{HI}} > 15.5$  somewhat better; for smaller values of  $N_{\text{HI}}$  the differences between the two runs are negligible.

In Fig.2 we show a temperature map from a slice through the high-res box at  $z = 3.27$ . Hot bubbles ( $T \simeq 10^6 \text{ K}$ ) of shocked gas produced by outflows around the parent galaxies are clearly apparent. Their sizes range from  $\approx 0.5 \text{ Mpc } h^{-1}$  to  $\approx 2 \text{ Mpc } h^{-1}$ , and their shape appears in some case rather jagged as a result of the interaction with the inhomogeneous ambient medium. The volume filling factor of gas with temperature above  $10^5 \text{ K}$  is 14%. The internal structure of the bubbles can be inspected more quantitatively in Fig.3, where the comparison between **sph** and **mfb** is shown (low-res case) for various physical quantities (hydrogen density,  $n_{\text{H}}$ , ionization fraction,  $x_{\text{HI}}$ , gas temperature,  $T$ , and peculiar velocity,  $v_{\text{pec}}$ ) along the LOS through the center of the most massive galaxy  $M = 1.5 \times 10^{11} M_{\odot} h^{-1}$  in these simulations; the galaxy position corresponds to the density peak at  $x \approx 6.8 \text{ Mpc } h^{-1}$ . In both simulations the star formation rate in this galaxy is  $5.6 M_{\odot} \text{ yr}^{-1}$  ( $18 M_{\odot} \text{ yr}^{-1}$ ) for the **mfb** (**sph**) models. A striking result of the comparison between the two models shows that, although outflows are able to heat the halo/IGM gas up to high temperatures out to more than  $1 \text{ Mpc } h^{-1}$  from the galaxy, they do not seem able to modify its density structure in a sensible way. Hence

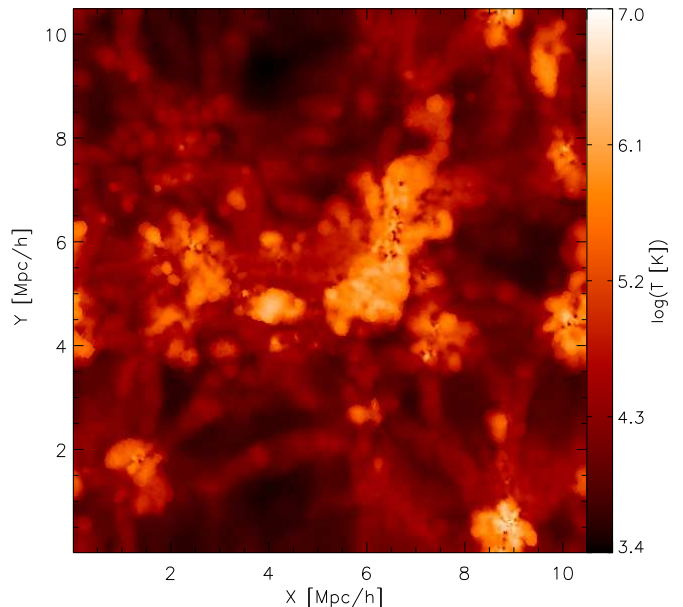


**Figure 2.** Temperature map in a slice through the high-res simulation box ( $z = 3.27$ ). The color bar shows the values of  $\log T$ .

the density in the surroundings remains high and close to that set up by the process of galaxy formation. Close to the galactic center the outflow peak speed is about  $130 \text{ km s}^{-1}$ , but this value rapidly decreases as kinetic energy is used to counteract the pressure of intergalactic accreting gas, raining onto the galaxy at essentially the escape speed of the system, roughly  $150 \text{ km s}^{-1}$ . The stalling radius is seen at the zero-crossing of  $v_{\text{pec}}$ , approximately  $0.3 \text{ Mpc } h^{-1}$  away from the outflow source. The relative insensitivity of the density to the SN energy injection can be interpreted as the fact that the outflow velocities are lower than the escape speeds and hence the flow is confined by inflow. Also, we note that the outflow velocities we find are lower than those inferred by A02,  $\approx 600 \text{ km s}^{-1}$  from LBGs.

Fig.4 shows the mean Ly $\alpha$  forest flux averaged on pixels on different LOS at different distances,  $\Delta r$ , from the galaxy centers in the simulation box, following the same experimental procedure as in A02:

$$\langle F(\Delta r) \rangle = \frac{1}{N(\Delta r)} \sum_{i=1}^{N(\Delta r)} F_i, \quad (2)$$

where  $N(\Delta r)$  is the number of pixels that fall in the bin  $\Delta r$ , and  $F_i$  is the transmitted flux in the pixel  $i$ . The synthetic data, normalized to the observational ones, are plotted only out to a distance  $\Delta r \approx 3.81 \text{ Mpc } h^{-1}$  for the low-res simulations ( $\Delta r \approx 5.32 \text{ Mpc } h^{-1}$  for high-res one) due to the periodic boundary conditions of the simulation. We first compare the two low-res **sph** and **mfb** cases. The difference between these curves is negligible and on average the Ly $\alpha$  absorption is similar: this is expected after the results analyzed in Fig. 1. In addition both simulations are

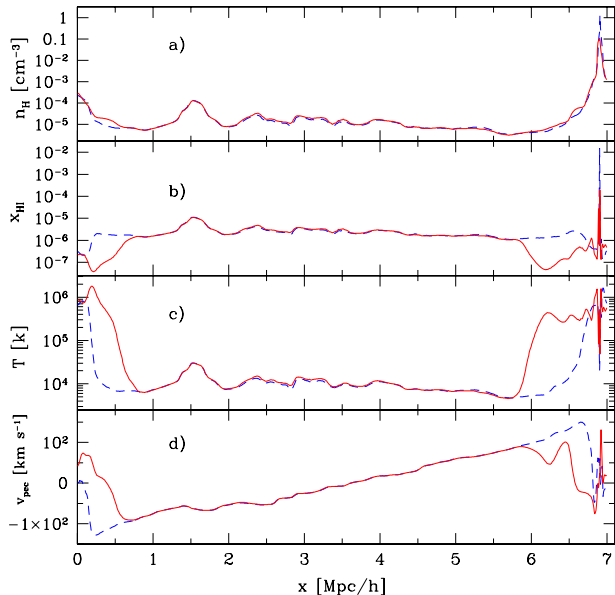


**Figure 3.** Comparison between *sph* (dashed line) and *mfb* (solid line) low-res runs along the LOS through the center of the most massive galaxy ( $M = 1.5 \times 10^{11} M_{\odot} h^{-1}$ ) whose position corresponds to the density peak at  $x \approx 6.8 \text{ Mpc } h^{-1}$ : *a*) hydrogen density, *b*) neutral hydrogen fraction, *c*) gas temperature, *d*) gas peculiar velocity.

in agreement with the high-res one, thus ensuring that numerical convergence has been reached and results are not affected by spurious effects. However, these models fail in reproducing the observed trend inside  $1 \text{ Mpc } h^{-1}$ . The simulated Ly $\alpha$  forest seems to be much more opaque than the observed one, with a maximum  $\tau$  discrepancy of about a factor 2.2. In order to assess if the disagreement could be reduced by a more efficient outflow clearing of the halos of smaller systems, we excluded the contribution of most massive galaxies ( $M > 1.5 \times 10^{10} h^{-1} M_{\odot}$ ) to the flux. However, as it is seen from the Figure, this does not solve the problem. As a final resort, we have randomized the position of galaxy centers in the box to account for the reported experimental error determination. To this aim we have added a gaussian random displacement to the redshift of each galaxy with r.m.s.  $\sigma_z = 0.002$ , which represents the  $1\text{-}\sigma$  error of the measure. This procedure improves the result, as now galaxy centers do not perfectly coincide with density peaks, but to an extent insufficient to explain the data.

## 4 CONCLUSIONS

Motivated by the recent observational results of A02, we have studied, with the help of a set of cosmological simulations including star formation in multiphase gas and outflows from galaxies, the effects of galaxy formation/activity on the properties of the surrounding Ly $\alpha$  forest. Although on large scales our simulations can reproduce remarkably well a number of statistical properties of the IGM, they fail to predict the observed Ly $\alpha$  flux increase in regions close to

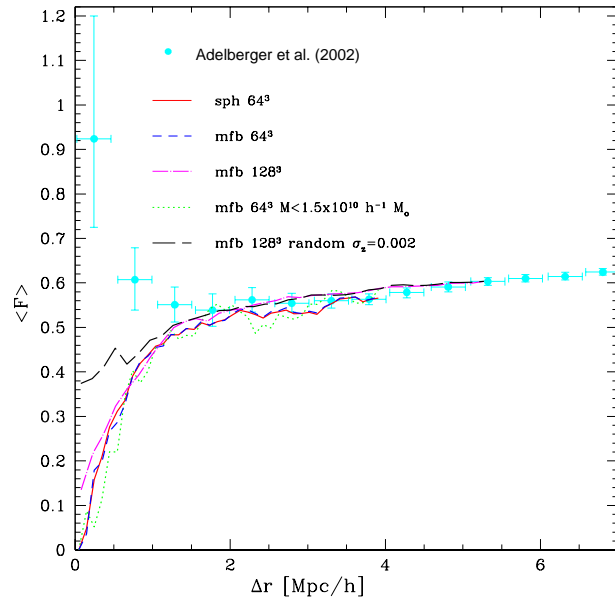


**Figure 4.** Mean Ly $\alpha$  forest flux at different distances  $\Delta r$  from the galaxies in the simulation box. Synthetic results are shown for five cases: low-res *sph* (solid line) and *mfb* (dashed); low-res *mfb* with least massive ( $M < 1.5 \times 10^{10} h^{-1} M_{\odot}$ ) galaxies only (dotted); high-res *mfb* (dot-dashed); high-res *mfb* with randomized galaxy centers (long-dashed). The points are the observational results by A02 for LBGs. Normalization to the data at large  $\Delta r$  has been performed (see text).

the galaxies themselves. The success can be ascertain to two concomitant effects: (i) outflows preferentially expand in regions of low-density (voids) thus preserving the filaments responsible for the Ly $\alpha$  absorbing network; (ii) the hot bubbles fill a relatively small fraction of the cosmic volume ( $\approx 14\%$  in our simulations). Support to the first hypothesis emerges also from an inspection of the velocity field in the surrounding of the most massive galaxy in the simulation: the inflow of gas from low density regions is blocked by the bubble expansion, but it proceeds basically unimpeded along the filaments (see Marri *et al.* 2003).

Much more puzzling is instead the reason for the opacity excess (with respect to real data) we see in the simulation in the inner  $\text{Mpc } h^{-1}$ . Apparently, simulated outflows do not carry sufficient momentum to disperse the density peak created in the vicinity of the galaxy as a leftover of its formation. Also, a large fraction of the outflow energy is used to counteract the infalling gas ram pressure which tends to pile up the gas into the galaxy. The temperature increase close to galaxies amplifies the magnitude of the collisional ionization rate, which becomes larger than the equivalent photoionization rate for  $T \gtrsim 10^5 \text{ K}$ . In this case the H I neutral fraction  $x_{\text{HI}}$  is independent of gas density and remains at roughly the same level as in the general IGM. Therefore, collisional ionization is not sufficient to balance the opacity increase induced by the density raise and the transmitted flux drops accordingly to the latter. What are the possible alternative explanations for the observed flux trend? The presence of a bias in the data produced by a preferential selection effect

of low Ly $\alpha$  absorption LBGs has already been suggested by Croft *et al.* (2002). Another possibility is provided by photoionization, particularly if one recalls the recent results by Steidel, Pettini & Adelberger (2001), who detected flux beyond the Lyman limit (with significant residual flux at  $\lambda < 912 \text{ \AA}$ ) in a composite spectrum of 29 LBGs at  $z = 3.4$ , a clue of a conspicuous escape probability of ionizing radiation from these objects. As mentioned above, the A02 data would require an optical depth (or equivalently a  $x_{\text{HI}}$ , assuming a prescribed density profile) a factor  $\approx 2-3$  smaller. If this can be achieved with the ionizing flux coming from galaxies must be proved with detailed radiative transfer calculations which are currently ongoing (Maselli *et al.* 2003) The first attempt using simplified analytical and/or post-processing techniques to account for this effect (Croft *et al.* 2002, Kollmeier *et al.* 2002) have yielded so far negative answers, but a fully self-consistent, physically accurate description of the problem is awaited in order to draw a final conclusion.

This work was partially supported by the Research and Training Network ‘The Physics of the Intergalactic Medium’ set up by the European Community under the contract HPRN-CT2000-00126 RG29185. MB thanks P.Petitjean for discussions and hospitality at IAP. We are grateful to S. Bianchi for help with AUTOVP and discussions.

## REFERENCES

- Adelberger, K. L., Steidel, C. C., Shapley, A. E. & Pettini, M. 2002, astro-ph/0210314
- Croft R.A.C., Hernquist L., Springel V., Westover M. & White M. 2002, astr-ph/0204460
- Ferrara, A., Pettini, M., & Shchekinov, Y. 2000, MNRAS, 319, 539
- Haardt F. & Madau P. 1996, ApJ, 461, 20
- Hu E.M., Kim T., Cowie L., Songaila A. & Rauch M. 1995, Astron. J., 110 (4), 1526
- Kollmeier, J., Weinberg, D. H., Davé, R. & Katz, N. 2002, astro-ph/0209563
- Mac Low, M-M. & Ferrara, A. 1999, ApJ, 513, 142
- Madau, P., Ferrara, A., & Rees, M. J. 2001, ApJ, 555, 9
- Marri, S., Ferrara, A., Bruscoli, M., Schneider, R. & Maselli, A., 2003, in preparation
- Marri, S. & White, S. D. M. 2002, astro-ph/0207048
- Maselli, A., Ferrara, A., Marri, S., Bruscoli, M. & Schneider 2003, in preparation
- McDonald *et al.* 2000, ApJ, 543, 1
- Petry C.E., Impey C.D., Katz N., Weinberg D.H. & Hernquist L.E. 2002, ApJ, 566, 30
- Rauch M. *et al.* 1997b, ApJ, 489, 7
- Rauch M., Haehnelt M.G. & Steinmetz M. 1997a, ApJ, 481, 601
- Savaglio S., Panagia N. & Padovani P. 2002, ApJ, 567, 702
- Scannapieco, E., Ferrara, A. & Madau, P. 2002, ApJ, 574, 590
- Steidel, C. C., Pettini, M. & Adelberger, K. L. 2001 ApJ, 546, 665
- Springel V., Yoshida N. & White S.D.M. 2001, NewA, 6, 79
- Theuns T., Leonard A., Efstathiou G., Pearce F.R. & Thomas P.A. 1998, MNRAS, 301, 478
- Theuns T., Viel M., Kay S., Schaye J., Carswell R.F. & Tzanavaris P. 2002, astro-ph/0208418